Cell-Sensitive Microscopy Imaging for Cell Image Segmentation

Zhaozheng Yin[1,⋆], Hang Su[2], Elmer Ker[3], Mingzhong Li[1], and Haohan Li[1]

[1] Department of Computer Science, Missouri University of Science and Technology
[2] Department of Electronic Engineering, Shanghai Jiaotong University
[3] Department of Orthopedic Surgery, Stanford University

Abstract. We propose a novel cell segmentation approach by estimating a cell-sensitive camera response function based on variously exposed phase contrast microscopy images on the same cell dish. Using the cell-sensitive microscopy imaging, cells' original irradiance signals are restored from all exposures and the irradiance signals on non-cell background regions are restored as a uniform constant (i.e., the imaging system is sensitive to cells only but insensitive to non-cell background). Cell segmentation is then performed on the restored irradiance signals by simple thresholding. The experimental results validate that high quality cell segmentation can be achieved by our approach.

1 Introduction

Phase contrast microscopy imaging [14], a non-invasive technique, has been widely used to observe live cells without staining them. The imaging system consists of a phase contrast microscope and a digital camera to record time-lapse microscopy images on cells to analyze their properties. As shown in Fig.1, the illuminance (L) passes through a Petri dish culturing cells and microscope optics, and generates the irradiance (E) observable by human eyes or digital cameras. The camera captures the irradiance (E) within an exposure duration (Δt) and transforms the accumulated irradiance (X, $X = E\Delta t$) into pixel values (I) in digital images by a CCD sensor response function f, i.e., the pixel value in a microscopy image is a function of irradiance and exposure time: $I = f(E\Delta t)$.

To automatically process cell images by computational algorithms, cell segmentation plays a key role because cells need to be segmented and localized in images first before being tracked and analyzed over time [3,8]. Well-known image segmentation algorithms such as thresholding, morphological operations, watershed, level-set and Laplacian-of-Gaussian filtering, have been explored in various cell image analysis systems [2,5,7,9,11,12]. Since these cell segmentation algorithms overlook the specific image formation process of phase contrast microscopy, recently the imaging model of phase contrast microscope optics and its related features have been exploited to facilitate the cell segmentation [10,13].

⋆ This research is supported by NSF CAREER award IIS-1351049, University of Missouri Research Board, ISC and CBSE centers at Missouri S&T.

P. Golland et al. (Eds.): MICCAI 2014, Part I, LNCS 8673, pp. 41–48, 2014.

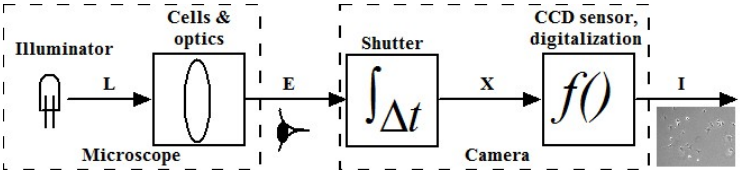

Fig. 1. Microscopy image formation process

However, the work on imaging model of phase contrast optics [13] focuses on the front-end of the entire imaging pipeline but ignores the rear-end (camera) of the pipeline. In fact, different camera settings also affect the cell image analysis. As shown in Fig.2, on the same cell dish, too short or too long exposure duration yields under-exposure (Fig.2(a)) or over-exposure (Fig.2(c)), respectively. Biologists and algorithm developers usually use a single suitable exposure (e.g., Fig.2(b)) to observe cells and analyze their images.

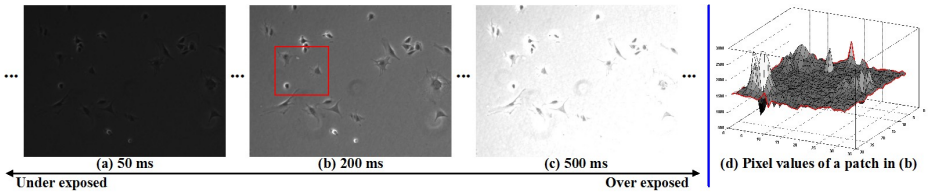

Fig. 2. (a,b,c): Multiple exposures on the same cell dish (ms: millisecond); (d): The pixel values of an image patch in (b) visualized in a surface view

Based on the phase contrast imaging pipeline and observation on differently exposed images, we are motivated to think of two intriguing problems in microscopy imaging and cell image segmentation:

- Biologists and algorithm developers aim to analyze cells' original properties encoded in the irradiance signal E. However, the camera response function f is usually nonlinear [1,4], i.e., the acquired image signal I is not linearly proportional to cells' irradiance E. Therefore, all cell image analysis algorithms directly based on image signal I may deviate from the expected analysis on cells' original physical properties encoded in E. *Can we restore the irradiance signal E from the image signal I for cell signal analysis?*
- During the microscopy imaging, we hope to have high-quality images on cells only without any noise from the culturing dish. But, the pixels of non-cell regions in a dish may exhibit a significant amount of noise as shown in Fig.2(d), causing a nonuniform background and low contrast between cell and background pixels. *Can we create a microscopy imaging system that is only sensitive to cells' irradiance (i.e., insensitive to background, with a constant irradiance signal on non-cell background regions, facilitating the cell segmentation task)?*

We propose to create a *cell-sensitive microscopy imaging* system by considering the rear-end of the imaging pipeline. First, multiple microscopy images with various exposure durations are taken on the same cell dish. Then, the camera response function is estimated from the set of multiple exposed images with a constraint that the irradiance signals of non-cell background pixels should be a constant. Therefore, the imaging system is virtually sensitive to cells only. Finally, the irradiance signal map of cells is restored from all exposures based on the cell-sensitive camera response function. In the restored irradiance signal map, non-cell background region has a constant irradiance different from those of cells, which facilitates cell segmentation by simple thresholding.

2 Methodology

Since cells migrate slowly in a dish, phase contrast images are usually taken every 5 minutes to monitor the cells' proliferation process over weeks. In our cell-sensitive imaging, the process to take multi-exposure images every 5 minutes with a range of known exposure durations ([50, 100, 200, 300, 400, 500]ms, in toal, about 1.55 seconds per set) is very fast compared to the time-lapse interval (5 minutes), hence the irradiance signal for each pixel is stable when capturing a set of multiple exposures and there is no need to do any image registration due to cells' slow motion. Common image acquisition software such as Axiovision 4.7 from Zeiss in our lab can routinely capture the multi-exposures every 5 minutes.

In this section, first we introduce how to estimate the cell-sensitive camera response function, based on which we then describe how to restore the irradiance signal with uniform background. Finally, we present how to perform easy cell segmentation on the restored irradiance signal map by simple thresholding.

2.1 Estimate the Cell-Sensitive Camera Response Function

Let E_i be the irradiance at the i_{th} pixel location in a cell dish. I_{ij}, the intensity of the i_{th} pixel in the j_{th} image with exposure duration Δt_j, is computed by

$$I_{ij} = f(E_i \Delta t_j) \tag{1}$$

where f is the camera response function (monotonic and invertible). Computing the inverse function of Eq.1 and taking the logarithm on both sides, we have

$$\log f^{-1}(I_{ij}) = \log E_i + \log \Delta t_j. \tag{2}$$

We formulate a constrained least square minimization problem to solve the unknown camera response function and irradiance signal

$$O(g, E) = \sum_{i=1}^{N} \sum_{j=1}^{P} \{\omega(I_{ij})[g(I_{ij}) - \log E_i - \log \Delta t_j]\}^2$$

$$+\alpha \sum_{i\in[1,N],\ i\in\Psi} (\log E_i)^2$$
$$+\beta \sum_{I=I_{min}+1}^{I_{max}-1} [\omega(I)g''(I)]^2 \quad (3)$$

where $g = \log f^{-1}$. Note that, we only need to estimate a look-up table for the function g since its input domain is the pixel value range. For a 12-bit TIFF image, the look-up table's length is 4096 with the minimum pixel value $I_{min} = 0$ and the maximum $I_{max} = 4095$. N and P denote the number of pixels and exposed images, respectively. The first term in Eq.3 is the data-fitting cost. The second term in Eq.3 is the regularization cost which enforces the logarithm of background irradiance to zero. Ψ is a set of some background pixel samples (to be explained later). The third term in Eq.3 is a smooth term avoiding overfit on the data, which is defined by curvature approximated by the second order numerical derivative, i.e., $g''(I) = g(I-1) - 2g(I) + g(I+1)$. In phase contrast images, the objects-in-interest (cells) are either dark or bright while the background pixels have a broad value range in the middle. Therefore, we use a weight function $\omega(I)$ to emphasize more on the two ends of the camera response curve (i.e., sensitive to cells) and less on the middle (i.e., to have a flat background region): $\omega(I) = |I - \frac{I_{min}+I_{max}}{2}|$. α and β in Eq.3 are coefficients to balance the three cost terms. In our experiments, we choose fixed coefficients with $\alpha = 1000$ and $\beta = 100$.

Since the objective function in Eq.3 is quadratic, taking its derivatives regarding to g and E and setting them to zero lead to an overdetermined system of linear equations ($\mathbf{Ax} = \mathbf{b}$) which can be solved using the pseudo inverse or singular value decomposition method. The unknown variable in the linear equation system is $\mathbf{x} = [g(I_{min}), ..., g(I_{max}), \log E_1, ..., \log E_N]$ whose first part is the cell-sensitive camera response function, a look-up table. Given N pixels from P multi-exposed images, we have $(I_{max} - I_{min} + 1) + N$ unknown variables in $\mathbf{x}$. To avoid rank deficiency in the linear equation system, we need $NP > I_{max} - I_{min} + 1 + N$. For our experiments, $P = 6$, $I_{min} = 0$ and $I_{max} = 4095$. We choose $N = 1000$ to satisfy this requirement.

We uniformly divide the image coordinate into 100 rectangular regions (a 10x10 grid). Within each region, we select 10 pixels whose values are evenly distributed from the minimum to the maximum in this region. In total, we obtain 1000 sample pixels some of which will be on the background. Then, we manually pick some (e.g., 50) pixels out of background samples as the set Ψ used in the regularization of Eq.3. Note that, there is no need to select all background pixels for the regularization. A small set of representatives will be enough to estimate the cell-sensitive camera response curve.

Fig.3(a) shows the estimated cell-sensitive camera response function (black curve) from a set of multiple exposed images. The samples from different exposed images (marked by circles with different colors in Fig.3(a)) cover different portions of the camera response curve. Given a fixed camera and culturing dish, the response curve only needs to be estimated once using the first set of multiple

exposed images and then it can be applied to successive sets of multi-exposures for time-lapse irradiance signal restoration. As shown in Fig.3(b), the cell-sensitive response curve is estimated every 1 hour using images from a 5-hour time-lapse cell image sequence, and the six curves overlap each other pretty well. Different cameras and culturing dishes may have different cell-sensitive response curves, as shown in Fig.3(c) which includes three slightly different response curves on three different dishes.

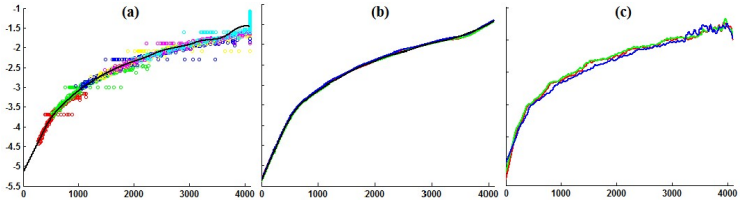

Fig. 3. Camera response curves. (a) The camera response function (black curve) estimated from multi-exposures on the same cell dish. The circles shown with different colors represent samples from different exposed images. (b) The response function of a camera estimated from six sets of multi-exposures captured every 1 hour on the same cell dish. (c) The response function of a camera estimated from three different dishes.

2.2 Restoring the Irradiance Signal

After the cell-sensitive camera response function is estimated from the first set of multi-exposed images, for any other sets in the time-lapse image sequence, we can easily restore their relative irradiance signals from image pixel values by

$$\log E_i = \frac{\sum_{j=1}^{P} w(I_{ij})(g(I_{ij}) - \Delta t_j)}{\sum_{j=1}^{P} w(I_{ij})} \tag{4}$$

where all the exposures are used to restore the irradiance signal robustly.

2.3 Cell Segmentation

Fig.4(a) shows an example of restored irradiance signal map whose surface view (Fig.4(b)) clearly shows that the non-cell background region has uniform background and the contrast between cells and background in the restored irradiance signal map is high. We sort the irradiance values in an ascent order (Fig.4(c)). The majority of the 1.5 million pixels of a 1040x1392 signal map has $E = 1$ (i.e., $\log E = 0$ which is the goal of regularization term in Eq.3).

In phase contrast microscopy imaging there are mainly three types of pixels: background pixels; bright pixels (e.g., mitosis/apoptosis cells or halos [6]); and dark pixels (e.g., migration normal cells [6]). Background pixels are commonly brighter than normal cell pixels but darker than bright pixels, as shown in Fig.4(a) and (b). The three types of pixel patterns are also reflected in Fig.4(c)

where the majority flat region of the curve belongs to background pixels while the low and high ends of the curve are contributed by the dark and bright cells, respectively. Two thresholds (T_H and T_L) are sufficient to segment cells out of the restored irradiance signal: any E signal larger than T_H is a bright pixel and any E signal lower than T_L is a dark pixel. Fig.4(d) shows the segmentation results of Fig.4(a). T_H and T_L are determined by basic grid search (comparing the segmentation accuracy of our method with the ground truth using different T_H's and T_L's). Given a time-lapse sequence, the thresholds are searched at the first time instant and then applied to all others.

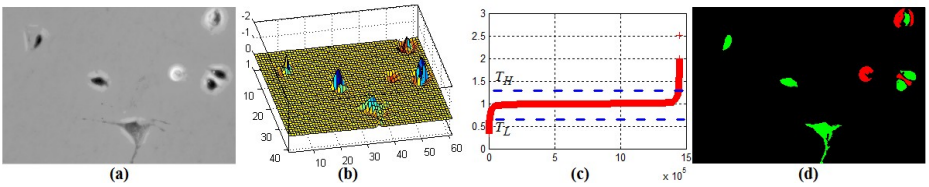

Fig. 4. Cell segmentation. (a) Restored irradiance signal map with constant irradiance values on the background and high signal contrast; (b) Irradiance map shown in the surface view. (c) The sorted irradiance signal values (red crosses). (d) Segmentation by thresholding the irradiance signal (green: dark cell pixels; red: bright cell pixels).

3 Experimental Results

We collected multiple exposed microscopy images on three different cell dishes with low and high cell densities, and each set has 6 different exposure durations ([50 100 200 300 400 500]ms).

3.1 Qualitative Evaluation

Multi-exposures have been used in Computer Graphics to create High Dynamic Range (HDR) images [1,4]. Fig.5 (b) shows the HDR image created by using the code from [1]. Compared to the image with 200ms exposure duration (Fig.5(a)), the HDR image shows more image details but also amplifies the background noise largely. However, our cell-sensitive imaging is only sensitive to cells and enforces the background to have a constant irradiance, showing high contrast between cells and the uniform background, as shown in Fig.5(c).

Fig.6 shows the qualitative comparison between our segmentation based on cell-sensitive imaging and two other related methods: (1) the phase contrast optics based method that considers the front-end of the imaging pipeline [13] and multi-level Otsu thresholding method [7]. Our restored irradiance signal map (Fig.6(a)) has uniform background and high contrast between cells and background regions. Thresholding the irradiance signals can classify both normal cells and bright cells (Fig.6(b)). The other two methods are ran on the image with exposure duration 200ms. The phase contrast optics based method can

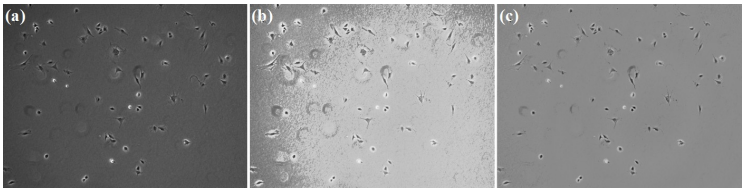

Fig. 5. Comparison with high dynamic range (HDR) image. (a) A phase contrast image captured with exposure duration 200ms. (b) The HDR image created by multi-exposures. (c) Our cell-sensitive imaging where the background is uniform and the image contrast between cells and the background is high.

locate the darkest nuclei regions but the low contrast cells and bright cells are not detected (Fig.6(c)). Considering there are three types of pixels in an image (bright cells, dark cells and background), we use two-level Otsu thresholding to segment the image. Unfortunately, the multi-level Otsu thresholding does not perform well due to the non-uniform background (Fig.6(d)).

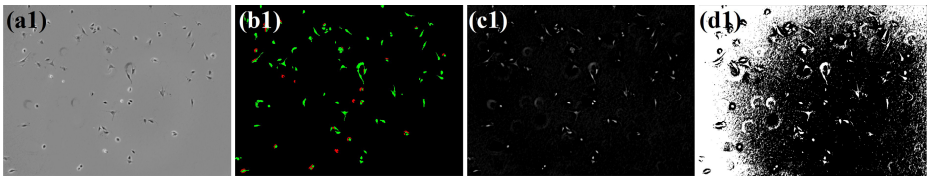

Fig. 6. Three methods on one dish sequence. (a) Restored irradiance signal by our cell-sensitive imaging. (b) The segmentation by thresholding the restored irradiance (red: mitosis/apoptosis cells or halos; green: normal migration cells). (c-d): Segmentation on the image with 200ms exposure duration by the method based on phase contrast optics model [13] and Otsu thresholding [7], respectively.

3.2 Quantitative Evaluation

Two annotators manually labeled cell masks (both mitosis/apoptosis and normal cells but without halos) in all microscopy images with exposure duration 200ms. To reduce the inter-person variability, the intersection of their annotations is used as the ground truth. The segmentation accuracy (ACC) is defined as $ACC = (|TP| + |N_s| - |FP|)/(|N_s| + |P_s|)$ where cell and background pixels are defined as positive (P_s) and negative (N_s) samples, respectively. True positive (TP) stands for cell pixels segmented by our method correctly and false positive (FP) denotes cell pixels segmented by our method mistakenly. Table 1 compares the performance of three segmentation methods on three cell sequences in which our segmentation by cell-sensitive imaging achieves very high accuracy. We did not classify bright halos from bright mitosis/apoptosis cells in this paper, which lowers our cell segmentation performance a bit. In the future work, we will explore cell classification and tracking based on the cell-sensitive imaging.

Table 1. Cell segmentation accuracy of three methods on three dishes

	Dish 1	Dish 2	Dish 3
Our cell-sensitive imaging	0.993	0.994	0.975
Optics model based method [13]	0.974	0.974	0.956
Otsu threshold [7]	0.677	0.665	0.628

4 Conclusion

We propose a novel cell segmentation approach by creating a cell-sensitive microscopy imaging system. A set of variously exposed phase contrast microscopy images on the same cell dish are used to estimate a cell-sensitive camera response function, based on which cells' original irradiance signals are restored from all exposures while the irradiance signals on non-cell background regions are restored as a uniform constant. Therefore, the imaging system is sensitive to cells but insensitive to non-cell background, which greatly facilitates the cell segmentation by simple thresholding. The experimental results show our approach can achieve high cell segmentation accuracy.

References

1. Debevec, P., Malik, J.: Recovering High Dynamic Range Radiance Maps from Photographs. In: SIGGRAPH (1997)
2. House, D., et al.: Tracking of Cell Populations to Understand their Spatio-Temporal Behavior in Response to Physical stimuli. In: Workshop on MMBIA (2009)
3. Kanade, T., et al.: Cell Image Analysis: Algorithms, System and Applications. In: IEEE Workshop on Applications of Computer Vision (WACV) (2011)
4. Larson, G., et al.: A Visibility Matching Tone Reproduction Operator for High Dynamic Range Scenes. IEEE Tran. on Visualization and Computer Graphics 3(4), 291–306 (1997)
5. Li, K., et al.: Cell Population Tracking and Lineage Construction with Spatiotemporal Context. Medical Image Analysis (MedIA) 12(1), 546–566 (2008)
6. Murphy, D.: Fundamentals of Light Microscopy and Electronic Imaging. Wiley (2001)
7. Otsu, N.: A threshold selection method from gray-level histograms. IEEE Transactions on Systems, Man, and Cybernetics 9(1), 62–66 (1979)
8. Rittscher, J.: Characterization of Biological Processes through Automated Image Analysis. Annual Review of Biomedical Engineering 12, 315–344 (2010)
9. Smith, K., et al.: General Constraints for Batch Multiple-Target Tracking Applied to Large-Scale Video Microscopy. In: CVPR (2008)
10. Su, H., et al.: Cell Segmentation in Phase Contrast Microscopy Images via Semi-supervised Classification over Optics-related Features. MedIA 17(7), 746–765 (2013)
11. Wu, K., et al.: Live Cell Image Segmentation. IEEE Tran. on Biomedical Engineering 42(1), 1–12 (1995)
12. Yang, F., Mackey, M.A., Ianzini, F., Gallardo, G., Sonka, M.: Cell Segmentation, Tracking, and Mitosis Detection Using Temporal Context. In: Duncan, J.S., Gerig, G. (eds.) MICCAI 2005. LNCS, vol. 3749, pp. 302–309. Springer, Heidelberg (2005)
13. Yin, Z., et al.: Understanding the Phase Contrast Optics to Restore Artifact-free Microscopy Images for Segmentation. MedIA 16(5), 1047–1062 (2012)
14. Zernike, F.: How I discovered phase contrast. Science 121, 345–349 (1955)